coatings

MDPI

Review

Protruding Nanostructured Surfaces for Antimicrobial and Osteogenic Titanium Implants

Mohd I. Ishak [1,2,*], Xiayi Liu [1], Joshua Jenkins [1], Angela H. Nobbs [1] and Bo Su [1,*]

[1] Bristol Dental School, University of Bristol, Lower Maudlin Street, Bristol BS1 2LY, UK; liu.xiayi.2019@bristol.ac.uk (X.L.); joshua.jenkins@ubc.ca (J.J.); angela.nobbs@bristol.ac.uk (A.H.N.)
[2] Faculty of Engineering Technology, Universiti Malaysia Perlis (UniMAP), Perlis 13600, Malaysia
* Correspondence: irill.ishak@bristol.ac.uk (M.I.I.); b.su@bristol.ac.uk (B.S.); Tel.: +44-(0)-1173429584 (M.I.I.); +44-(0)-117 3424313 (B.S.)

Received: 2 July 2020; Accepted: 27 July 2020; Published: 3 August 2020

Abstract: Protruding nanostructured surfaces have gained increasing interest due to their unique wetting behaviours and more recently their antimicrobial and osteogenic properties. Rapid development in nanofabrication techniques that offer high throughput and versatility on titanium substrate open up the possibility for better orthopaedic and dental implants that deter bacterial colonisation while promoting osteointegration. In this review we present a brief overview of current problems associated with bacterial infection of titanium implants and of efforts to fabricate titanium implants that have both bactericidal and osteogenic properties. All of the proposed mechano-bactericidal mechanisms of protruding nanostructured surfaces are then considered so as to explore the potential advantages and disadvantages of adopting such novel technologies for use in future implant applications. Different nanofabrication methods that can be utilised to fabricate such nanostructured surfaces on titanium substrate are briefly discussed.

Keywords: nanostructured surfaces; antimicrobial; bactericidal; osteogenic; medical implants

1. Introduction

Medical implants are devices that are placed inside or on the surface of the body to replace or restore the function of damaged or degenerated tissues or organs. Each year, millions of patients benefit from medical implants that help to improve their quality of life by prolonging the functionality of important organs beyond their original lifespan. Other types of implants may also be utilised for delivering medication, monitoring patient bodily functions or providing support to organs and tissues [1].

The demand for medical implants is expected to increase due to an ageing population and changing lifestyle. Medical implants based on titanium metal and its alloy comprise the largest share of the market in orthopaedics, dentistry and cardiovascular surgery and are expected to continue as marker leaders due to their advantages such as good biocompatibility and excellent mechanical properties [2].

Because of the cost and complexity of the surgical procedure, many orthopaedic implants are designed to last approximately 20–25 years [3]. Every year, millions of patients undergo successful prosthetic joint replacement surgery, which restores biological function, relieves pain and improves or restores mobility [4]. However, complications arising from this surgery that require revision can account for up to 11% of cases after 15 years [5]. In 2018, revision surgeries for hip and knee implants were reported to be 10.8% and 6.5%, respectively. The National Joint Registry reported that revision surgery increases with time. For instance, the need for revision surgery for a hip implant in the first year is 0.78%. This increases to 1.54% in the third year and can be as high as 4.87% after 15 years.

Re-revision for implants that fail within the first year are twice as likely compared to those that last for more than five years.

Implant failures are multifactorial and can include host risk factors (e.g., pre-existing diseases, smoking and drinking habits, age, metabolic conditions), implantation factors, surgical procedures and implant properties [6]. Nevertheless, the two most prevalent causes of implant revision surgeries and failure are reported as infection and aseptic loosening, with the latter often resulting from an infection impairing osteointegration and so causing aseptic loosening [6].

Titanium dental implants are commonly used to treat missing teeth due to trauma, tooth decay or periodontal diseases [7,8]. Similar to orthopaedic implants, demand for dental implants has seen a rapid increase over the last decade [9]. Approximately 130,000 dental implants were inserted in the UK in 2012 and this figure doubled in 2018 [10]. Dental implants are expected to last over 10 years with a survival rate of 90–95% [11]. Current dental practices to reduce post-operative complications include evaluation of systemic or syndromic diseases, immune disorder [12] and accurate examination of the bone crest for proper implant fitting [13]. However, factors such as the dental implant properties (i.e., surface roughness, anatomic site and implant fit) and patient oral hygiene (i.e., periodontitis, bone quality, vascular integrity, soft tissue viability) will influence the risk of implant failure [11].

Biofilm Formation on Medical Implants

Despite many breakthroughs in science and technology, a significant proportion of medical implants are infected by bacteria. Implant infection is estimated to cause around a fifth of implant failures, which can occur at any time post-implantation but are most likely during the first year before substantial osteointegration has occurred. Commonly, there are three ways bacteria can infect an implant—during surgery, infection from neighbouring tissues or via the haematogenous route, where the bacteria are transferred to the implant site via the circulatory or lymphatic system. Orthopaedic implants can also cause bone-tissue conditions such as osteomyelitis and septic arthritis, which involve inflammatory destruction of joint and bone [14].

Staphylococci such as *Staphylococcus aureus* and *Staphylococcus epidermidis* account for most implant-related infections, being identified from two out of every three cases (Table 1) [14]. This is because *S. aureus* is known to have surface proteins with specific affinity for binding human targets like collagen, fibronectin and bone [4]. Enterococci cause <15% of implant infections, as do aerobic Gram-negative bacilli like *Escherichia coli, Klebsiella pneumoniae* and *Pseudomonas aeruginosa*. Around 1% of implant infections are caused by fungi, with most cases due to *Candida albicans*. Polymicrobial infections have been reported to account for approximately 15% of hip and knee implant infections.

After successful adhesion to the surface of the implant, bacteria will form a biofilm in which the cells proliferate within a protective layer of extracellular polymeric substances (EPS) consisting of polysaccharides, proteins, lipid and extracellular DNA [15]. Biofilms offer many benefits to the bacteria such as protection from the host immune response and antibiotics and allowing efficient communication and direct information exchange [16]. The EPS matrix can also promote a favourable adhesion environment for the bacteria on abiotic and biotic surfaces that is capable of shielding the bacteria from stresses such as osmolarity and pH changes, shear forces and UV radiation [17].

Conventionally, prosthetic joint infections are treated using antibiotic therapy and revision surgery. Antibiotic therapies often vary between patients with regards to types of antibiotics used, duration of therapy and route of administration and can be influenced by host risk factors and the type of revision surgery intervention [18]. However, the presence of a biofilm on the medical implant can often cause additional problems since the EPS matrix can provide a protective barrier that impairs antibiotic penetration into the biofilm. One approach to prevent biofilm formation on titanium implants involves applying a chemical surface coating that kills bacteria. This has been achieved using antibiotics, antimicrobial peptides and metal nanoparticles [6]. The antibacterial properties of silver are widely reported [19], with bactericidal activity observed against a broad range of bacteria, including *S. aureus*,

S. epidermidis, *E. coli* and *P. aeruginosa* [20]. The photocatalytic activity of anatase TiO_2 has also been utilized to enhance the bactericidal activity of titanium surfaces [21].

Furthermore, as bacteria proliferate within the biofilm, the concentration of nutrients and oxygen can start to deplete. To adapt to these conditions, bacteria at the centre of a biofilm can become dormant or grow at a slower rate. This process is often referred to as adaptive resistance and can further enhance antibiotic resistance of bacteria within the biofilm [22]. Several studies have shown that to effectively kill bacteria within biofilms, antibiotics have to be administered at 10–1000 times the effective concentration needed under planktonic conditions [23].

Table 1. Summary of biofilm-forming microorganisms commonly found on titanium medical implants.

Medical Implant Type	Microbes Found	References
Orthopaedic Implants	Coagulase-negative staphylococci, haemolytic streptococci, enterococci, Proteus mirabilis, Bacteroides species, Staphylococcus aureus, Escherichia coli, Pseudomonas aeruginosa	[24,25]
Replacement Joints	*S. aureus*, *S. epidermidis*	[26]
Cardiac Pacemakers	*S. aureus*	[24]
Dental Implants	Gram-positive cocci (e.g., Streptococcus), Gram-negative anaerobic oral bacteria	[24,26]

2. Prevention of Biofilm Formation Using Protruding Nanostructured Surfaces

Microbial adhesion is an essential step for bacterial colonisation and the formation of a biofilm. Experimental and theoretical studies have shown that prevention and inhibition of biofilm formation is possible by tuning the properties of the substrata, which will influence bacterial adhesion. Such properties include biological properties (conditioning layer), physicochemical properties (surface charge, pH, functional groups, hydrophobicity) [27] and surface topography (roughness, nano/microtopography or hierarchical topography). In recent years, there have been tremendous efforts made to understand and develop antimicrobial surfaces based on protruding nanostructures.

The idea of using protruding nanostructures to prevent bacterial infections and biofilm formation was inspired by nature. Protruding nanostructured surfaces were first exploited as antifouling surfaces due to their reported hydrophobic and superhydrophobic properties, as seen on lotus leaves, rose petals and shark skin [28]. Shark skin has been studied extensively and shows excellent antifouling properties against ectoparasites and *Ulva* spores. A commercially available biomimetic shark skin product called Sharklet AF™ has been shown to be effective in limiting bacterial contamination. Mann et al. reported a significant reduction in *S. aureus* (MSSA and MRSA variants) bound to the Sharklet AF™ surface compared to flat control and pure copper alloy surfaces [29]. Another study also found that the Sharklet AF™ surface can inhibit *S. aureus* biofilm formation, with only 35% of the microtopography surface covered by a biofilm after 21 days as opposed to 77% coverage on the flat surface [29]. Currently, this technology has been used on a foley urinary catheter, endotracheal tube, wound dressing and central venous catheters [30].

Despite promising results for the use of nanostructured surfaces as antifouling materials, there are some concerns with regards to applying this approach to implant surfaces. For instance, use of an antifouling surface on a medical implant may enhance bacterial colonisation of the surrounding tissues. Indeed, this has been reported with OptiChem®surface, where the surrounding tissues were colonised by *S. aureus* but not the hydrophobic polymer-coated surface [31]. Antifouling surfaces are also expected to inhibit the attachment [32] and migration of mammalian cells [33], which could compromise the fixation of implanted devices.

With growing concerns over the emergence of antimicrobial resistant bacteria, significant attention has been given to finding alternative solutions to kill bacteria without reliance on antibiotics. Ivanova et al. was first to report the bactericidal properties of protruding nanostructured surfaces found on the cicada wing against *P. aeruginosa* [34]. As opposed to natural antifouling surfaces that

are usually found on marine or aquatic organisms [35–37], natural bactericidal surfaces are mostly found on insect wings [34,38–41]. Several species of cicada [34,39] and dragonfly [38,40] have been shown to possess wings with bactericidal activity (Figure 1). Butterfly and moth eyes [41], as well as gecko skin [42], which all have distinct nanostructured surfaces, have also been reported to possess bactericidal properties. Several studies have shown similar or enhanced bactericidal effects mediated by biomimetic nanotopographies on synthetic materials [43–48]. A list of natural and synthetic bactericidal nanostructured surfaces can be found in recent reviews [49,50].

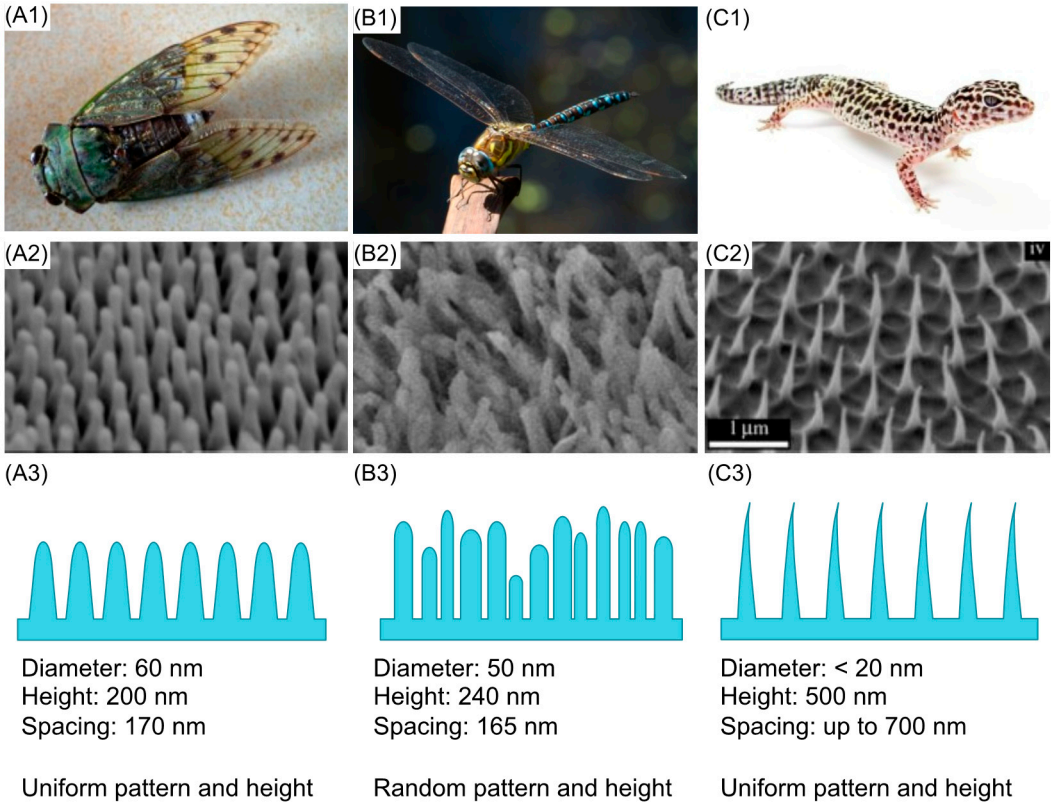

Figure 1. Naturally occurring mechano-bactericidal surfaces: (**A1**–**C1**) Cicada, dragonfly and gecko, respectively; (**A2**–**C2**) Scanning electron microscopy (SEM) images of cicada wing, dragonfly wing and gecko skin; (**A3**–**C3**) Schematic of the representative nanotopographies found on the cicada wing, dragonfly wing and gecko skin to highlight the differences between each nanotopography.

3. Understanding Bacteria–Nanostructure Interactions

3.1. Stretching and Mechano-Inducing Models

Several theoretical models have been proposed to explain the bactericidal mechanisms of protruding nanostructured surfaces. The first model compared the relatively uniform patterns and nanotopographies found across cicada wing-like surfaces with the more randomly oriented nanowires found on the surface of dragonfly wings. In general, Pogodin et al. proposed that bacterial cell lysis was due to the rupturing of the cell wall that was suspended between two adjacent nanopillars as opposed to a puncturing mechanism. The stretching of the cell wall in this region was significantly higher compared to a region that was directly adsorbed to the nanopillars, which led to rupturing of the membrane. This theory was consistent with a previous study which showed killing of *P. aeruginosa* by gold-coated cicada wing surfaces, implying that the bactericidal properties of the surfaces were not due to chemical or biochemical reactions. This theory also demonstrated that the bactericidal properties of the protruding nanostructured surfaces were dependent on the mechanical properties of the bacterial cell wall, which explained previous observations that killing by nanostructured surfaces was more

effective against the mechanically weaker cell wall of Gram-negative bacteria than the structurally more stable Gram-positive cell wall [51].

Two other mechano-bactericidal models based on the work by Pogodin et al. were then proposed to predict the efficacy of bactericidal properties as a function of nanotopography (i.e., tip diameter, nanopillar density, height) (Figure 2A). Both models proposed by Xue et al. and Li et al. further expanded the original model by including other parameters (e.g., gravity, Brownian motion, cell wall properties, free energy change of the cell wall) and using different approaches to predict the outcome. Xue et al. predicted that the mechano-bactericidal properties of cicada wing-like surfaces could be enhanced by increasing the sharpness and spacing of the nanopillars, which maximised the stretching of the envelope [52] (Figure 2B). Through quantitative thermodynamic studies, Li et al. proposed a phase diagram that highlighted ranges of different dimensions of nanopillar diameter and spacing and the resulting stretching of the bacterial envelope [53]. This study proposed the importance of adhesion energy and deformation energy to the bactericidal activity of nanostructured surfaces, indicating that stretching of the bacterial cell wall was significantly enhanced by nanopillars of 40 nm in diameter and a spacing of 100 nm (Figure 2C).

Several other papers have proposed models that use a different approach to Pogodin et al. For instance, Wu et al. compared experimentally and theoretically the effects of nanostructure density and height heterogeneity on the stretching degree of the bacterial cell envelope [54]. Four different scenarios were proposed, which showed that the stretching degree increases as the density increases (Figure 2D). Watson et al. proposed a much simpler model to explain the bactericidal mechanism of cicada wing-like surfaces based on changes in surface energy and considered several constraints for the optimal geometry of the nanopillars (e.g., radius, spacing and length) [55]. Changes in tensile strength were modelled as a function of cell wall thickness and it was found that tensile stress of the cell wall increases as the tip of the nanopillars increases (Figure 2E). Velic et al. used a two-dimensional finite element model to explain the interaction of *Bacillus subtilis* with a nanostructured surface [56]. Their model suggested that two key parameters for the bactericidal mechanism were nanopillar geometry and the interaction forces. It was found that stress on the cell wall reduces as the diameter increases and that stress increases when the interaction force increases. Their model also suggested that height variation between 200 to 500 nm has no significant effect on cell wall stress (Figure 2F). In a slightly different study, but still related to the biophysical model of bacteria-substratum interaction, a simulation study using the Extrand model revealed that bacterial adhesion to the surface may be reduced by tuning the protruding nanostructured surfaces [57].

Whilst undoubtedly useful, there are several limitations to the proposed models due to the complexity of bacterial-substrata interactions. Most importantly, all models assume that the bacterial cell wall is an elastic rather than a viscoelastic material for which deformation is not dependent on the applied force and time [58]. These models also disregard the importance of physicochemical properties of the bacterial cell wall, which has been highlighted in the extended Derjaguin-Landau-Verwey-Overbeek (DLVO-X) model used to predict bacterial adhesion to solid surfaces [59]. The specific interaction forces required to rupture the cell wall are currently unknown.

3.2. Other Possible Bactericidal Mechanisms

Alternative antimicrobial or bactericidal mechanisms of nanostructured surfaces have been proposed based on experimental observations. Bandara et al. suggested that shear forces might be involved in the bactericidal mechanism of high aspect ratio nanostructures (HARN) [40]. Since the height of HARN on dragonfly wings is not uniform, bacteria were found to first adhere to the tall nanospikes, which immobilised the cells. Shear force was then proposed to be generated by the lateral movement of the adherent bacteria that tried to evade the unfavourable surface. A 3D reconstruction of the focused ion beam SEM (FIB-SEM) data and transmission electron microscope (TEM) tomogram revealed that some of the nanospikes bent, causing the bacterial membrane to wrinkle and undergo blebbing (Figure 3A).

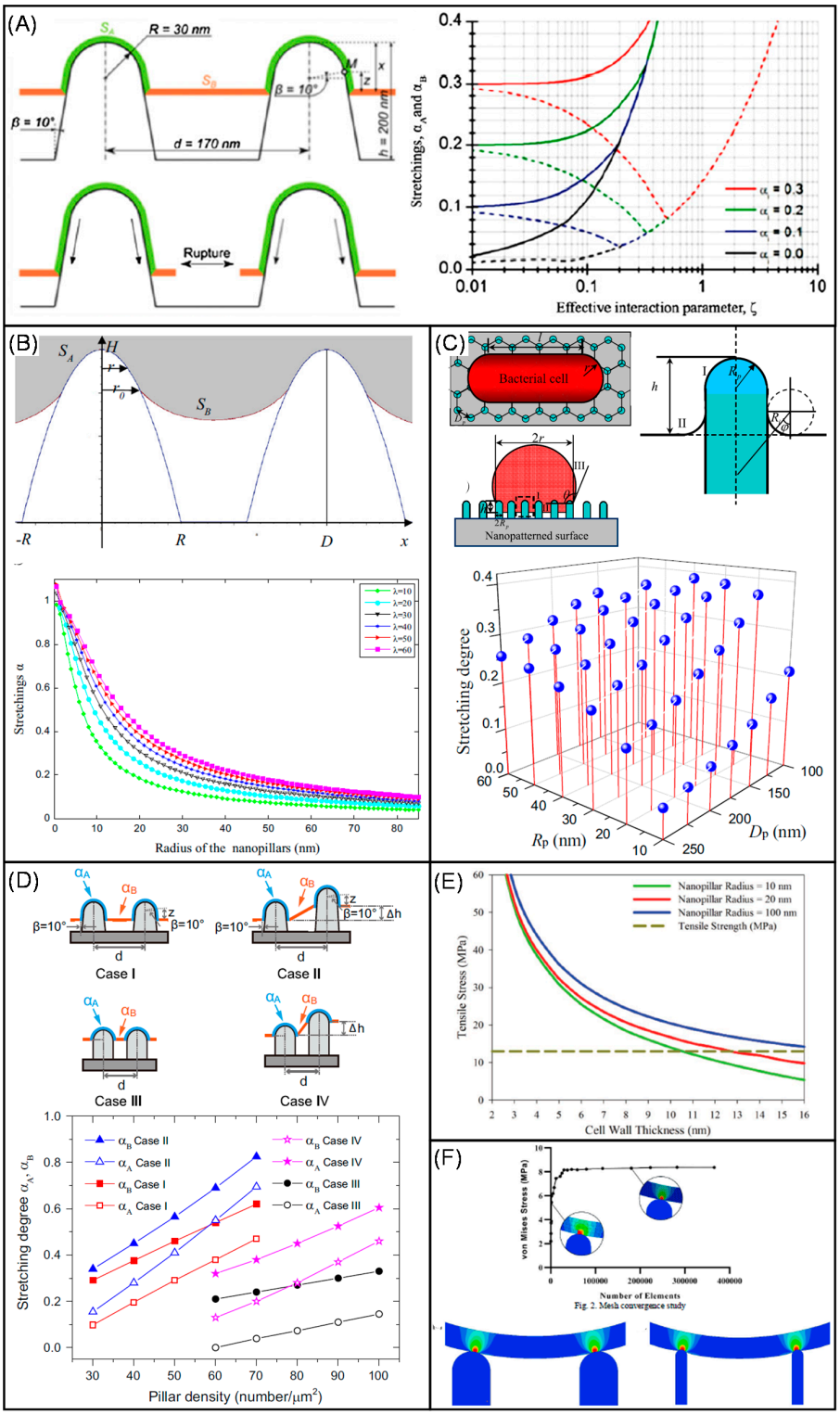

Figure 2. Current proposed theoretical models for the bactericidal mechanisms of nanotopographies analogous to those found on the cicada wing: (**A**) The first stretching model proposed by Pogodin et al. described rupturing of the cell membrane that was suspended between two adjacent nanopillars [reproduced with permission from Ref. [51]; (**B**) Xue et al. incorporated other geometric measurements of the nanopillars and parameters such as gravity and Van der Waals forces into the model. They found that stretching of the cell membrane increased as the radius of the nanopillars became smaller (i.e., sharper) [reproduced with permission from Ref. [52]; (**C**) Li et al. used a thermodynamic approach

to calculate the free energy change of the stretched cell membrane when adhered to a bed of nanopillars. A phase diagram based on this model was proposed, which showed that membrane stretching increased as the nanopillar density and sharpness increased [reproduced with permission from Ref. [60]; (**D**) Wu et al. incorporated the non-uniformity observed in some of the nanopillared surfaces into the model and proposed 4 different cases that might result in a different level of stretching. In all the cases, stretching degree increased as the density increased [reproduced with permission from Ref. [54]; (**E**) Watson et al. proposed a model that considered the binding behaviour of the cell to the nanopillars. Their model showed that the maximum tensile stress of the cell wall increased as the tip of the nanopillars increased [reproduced with permission from Ref. [55]; (**F**) Velic et al. developed a model to predict the deformation and stress contour of the cell wall when interacting with the nanopillars; Their model suggested that differences in height did not cause a differential in stress. Density showed small effects, while diameter of the pillars and interaction forces between the bacteria and the surface showed significant differences [reproduced with permission from Ref. [56].

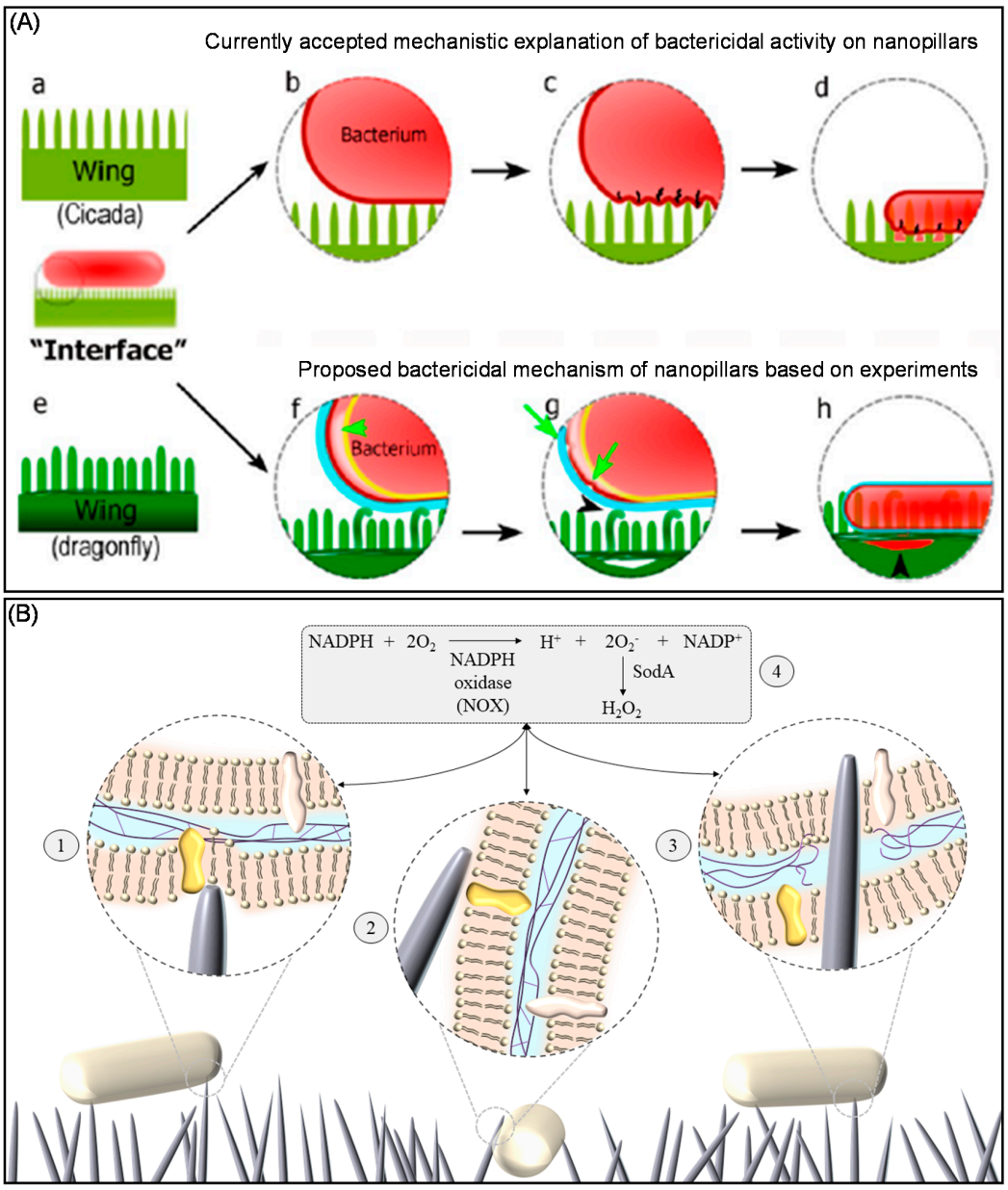

Figure 3. Proposed mechanisms of mechano-bactericidal surfaces. Current accepted bactericidal mechanisms based on cicada wing-like surfaces are shown in **A** (**a**–**d**). Since the height of nanopillars on the cicada wing is relatively uniform, there are multiple contact points between the bacterial membrane

and the surface upon adhesion. Due to interaction forces, the membrane stretches and eventually ruptures; **A** (**e**–**h**) show bactericidal mechanisms proposed for dragonfly wing-like surfaces, which consist of non-uniform high aspect ratio nanopillars, meaning that initial contact points are expected to be fewer than for the cicada wing. Interactions with bacteria cause the nanopillars to bend instead of puncturing or rupturing the bacterial membrane. Due to adhesion force, the cell membrane starts to wrinkle and form blebs, which eventually causes the cytosol to leak out [reproduced with permission from Ref. [40]]; (**B**) Proposed possible interrelated antibacterial mechanisms of nanopillared TiO_2 surfaces. (1) Some bacteria may experience cell membrane deformation when adhering between nanopillars, leading to cell impedance and impaired cell replication. (2) If the deformation reaches the elastic limit of the cell envelope, the nanopillars can penetrate the cell envelope. (3) The physiological interactions between bacteria and nanopillars can result in an oxidative stress response and induce the production of reactive oxygen species (ROS), leading to reduced bacterial growth and increased membrane susceptibility [reproduced with permission from Ref. [47]].

Jenkins et al. proposed that the antibacterial effects of protruding nanostructured surfaces are multifactorial [47]. TEM and FIB-SEM studies confirmed that nanospikes fabricated using a thermal oxidation method could induce cell deformation and penetration of the bacterial cell wall but it was found that these mechanical actions might not necessarily result in cell lysis. They also demonstrated entrapment of bacteria on HARN and subsequent impairment of cell proliferation. Another notable finding was that bacteria generated significant levels of reactive oxygen species (ROS) when on the nanostructured surfaces compared to the flat surface. This was further supported by comparing the proteomic response of *E. coli* and *S. aureus* exposed to a flat TiO_2 vs. nanostructured surface and the identification of elevated expression of several proteins associated with oxidative stress in the presence of nanospikes. Previous studies have reported that high concentrations of ROS could impair bacterial growth and biofilm formation [61,62], suggesting another potential mechanism by which the nanospikes mediate antibacterial effects.

4. Osteogenic Nanostructured Surfaces

Osteointegration, introduced by Branemark, refers to a direct and stable contact between implant and ordered bones [63]. It is of vital importance for achieving primary stability and long-term clinical success of medical implants. Osteointegration involves a series of molecular and cellular events that are strongly influenced by many factors, including implant characteristics (Table 2). For example, metal ions released from implant surfaces diffuse into surrounding tissue [64] and may affect protein expression of nearby cells [65]. Implant surface topography, including micro and nanotopography, had a strong influence on the healing events of osteointegration [66] (Table 2).

After implantation, early-stage tissue responses to the surgical trauma involve inflammation, cell adhesion and apoptosis. Titanium implants with 75 nm semispherical protrusions were reported to reduce initial inflammatory reactions via attenuated monocyte chemoattractant protein-1 (MCP-1) and tumour necrosis factor-α (TNF-α) expression in vivo [67]. Also, higher osteogenic activity (indicated by osteocalcin upregulation) and lower osteoclastic activity (indicated by reduced CatK expression) were detected for a group receiving implants with a nanostructured surface within a week of implantation [68]. Greater levels of osteoid and woven bone were found to form on the nanostructured surfaces compared with a flat surface. Alongside effects on inflammation, several studies have shown that nanotopographic features are able to modulate cell attachment. A study on pillar-like nanostructures indicated that cell focal adhesions and cell spreading decreased as nanostructures increased from 15 to 55 to 100 nm in height on Ti surfaces [69]. This result is consistent with studies using polymer surfaces with nanopillars or nanoislands, which have shown that the number of adherent cells and their dimensions reduce with rising height of the nanostructures [70,71].

After the immediate tissue response, effective bone mineralization between the bone/implant interface is required to achieve osteointegration. Dalby et al. [72] revealed that Human Bone Marrow

Cells (HBMCs) cultured on polymethyl methacrylate (PMMA) nanoscale islands and hemispheres increased expression of osteoblast markers osteocalcin (OC) and osteopontin (OPN) [73]. Their work indicated that nanoscale topographies, including nanoscale pit and heterogeneous islands, promoted pathways associated with skeletal development while suppressing those linked with connective tissue development. The targeted canonical pathways comprise actin, integrins, p38 mitogen-activated protein kinase (MAPK) and extracellular signal-regulated kinase (ERK). These results fit well with the observations by Yu et al. on nanoneedles formed on titanium substrate [74]. In another study, it was observed that 15 nm nanopillars enhanced phosphor-Runx2 (pS465) abundance, osteocalcin deposition and osteopentin by MSC cultures but these effects were significantly lower on a 90 nm substrate, indicating that adherent cells responded differently according to nanotopography [69,75]. Moreover, 15 nm highly disordered nanopillars on Ti substrate inhibited osteoclastogenesis, as indicated by upregulated osteoprotegerin (OPG) expression and reduced receptor activator of nuclear factor kappa-B ligand (RANKL) expression but promoted osteogenesis [76]. This favourable osteogenic characteristic reduced bone resorption during the bone remodelling process, making the protruding nanostructured surfaces ideal for developing orthopaedic implants. This is in contrast to the commercial titanium implant, for which it was found that RANKL is upregulated, which can be immunogenic and act as a secondary inflammatory stimulus in peri implantitis to amplify bone resorption [77].

Table 2. Summary of biological processes and molecules affected by nanotopography.

Influenced Process	Nanostructure	Related Genes/Pathways	References
Inflammation	Semispherical Protrusion	MCP-1 TNF-α	[67,68]
Cell attachment	Nanopillars Nanoislands	–	[69–71]
Osteogenesis	Nanoislands	Osteocalcin (OC), Osteopontin (OPN)	[69,72,73,75]
	Nanopillars	Actin, Integrin, p38 MAPK and ERK Pathways	
Osteoclastogenesis	Nanopillars	Osteoprotegerin (OPG), RANKL	[76]

5. Fabricating Bactericidal and Osteogenic Nanostructures on Titanium Surfaces

The translation from laboratory research findings to commercialised products is often difficult and many attempts end in failure [78]. This challenge is even greater for clinical applications, which have two "valleys of death"—upscaling of the products and clinical trials. For example, hundreds of promising antimicrobial technologies reported in the literature have failed in clinical testing and most have not even reached in vivo testing [79]. For many new technologies, ensuring fabrication protocols are efficient and, most importantly, cost effective [80] can be a major hurdle. Most nanofabrication protocols are very specific, expensive, have a low yield and often are not environmentally friendly. In this section, four promising nanofabrication techniques are reviewed that have potential to facilitate the translation of protruding nanostructured surfaces on titanium medical implants from lab bench to industry.

5.1. Hydrothermal Process

Hydrothermal process is one of the preferred techniques to fabricate nanostructures on titanium surfaces due to its simplicity, reliability and high throughput. It is also an environmentally friendly nanofabrication technique, which operates at a relatively low temperature, uses low concentrations of acids or bases and can use water as the reaction medium [81]. Hydrothermal offers a high degree of versatility in the final design of the nanotopography, which can be controlled by manipulating the experimental parameters such as operating temperature, reaction time, concentration of the rection media (e.g., acids or bases) or pre and post treatment of the substrate. It has also been used to generate nanostructures on different materials like zinc [82,83], barium [84–86], strontium [86–88] and

titanium [89–93]. Most importantly, hydrothermal process can be used to generate nanostructures on both 2D flat and different forms of 3D surfaces (e.g., mesh, wires, beads), which is desirable for the application of orthopaedic implants [94,95]. Some of the nanostructures generated to mimic the nanotopography found on dragonfly wings with a tapered end are shown in Figure 4A.

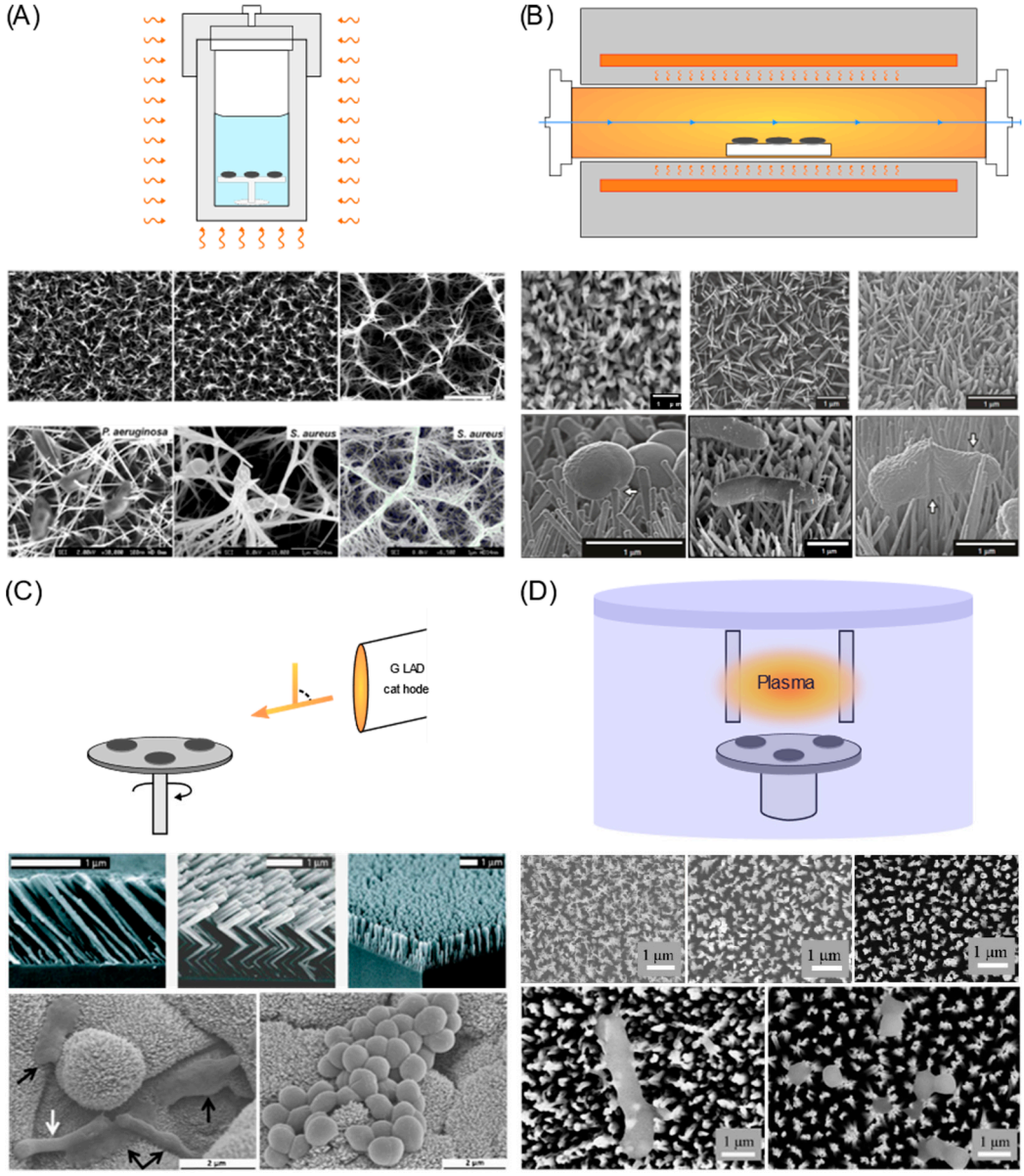

Figure 4. Nanofabrication techniques that offer excellent versatility and high throughput and the typical surface topographies generated: (**A**) alkaline hydrothermal (AH); (**B**) thermal oxidation (TO); (**C**) glancing angle deposition (GLAD) and (**D**) reactive ion etching (RIE). Each panel shows a basic schematic of the technique, an example of the protruding nanostructured surfaces generated by each technique and evidence of bactericidal activity.

The most common combination to generate protruding nanostructured surfaces on Ti and its alloy includes the use of an alkaline solution such as sodium or potassium hydroxide within an enclosed system at elevated temperatures; the so-called alkaline hydrothermal (AH) process. During this process, alkaline titanate nanostructures are generated first, followed by the substitution of alkali ions within the titanate with hydrogen ions to form hydrogen titanate through a post treatment with hydrochloric acid (HCl) and a final calcination step at 600 °C for the conversion to TiO_2 [89]. However, some studies

have shown that post heat treatments are not a prerequisite to acquire functional nanostructured surfaces [96].

There have been many studies that show the potential application of surfaces generated via the AH process. Two distinct nanostructures called the "brush" and "niche" type (height: >2 µm, diameter: 50 nm) have been shown to exhibit bactericidal activity against motile bacteria such as *P. aeruginosa*, *E. coli* and *B. subtilis*, while less significant effects were seen with non-motile *S. aureus, K. pneumoniae* and *Enterococcus faecalis* [43]. Shorter and sharper TiO_2 nanospikes (height: 1000 nm, diameter: 24 nm) fabricated via the AH process were found to kill up to 50% of the adherent bacteria after 1 h of incubation [92]. Tsimbouri et al. also reported promising osteogenesis and osteoclastogenesis properties of the surface. Shorter and slightly bigger nanospikes (height: 500 nm, diameter: 50 nm) were able to effectively inhibit the growth of *S. aureus* when incubated for 18 h. Human osteoblast cells also exhibited higher metabolic activity on this type of nanostructure compared to flat Ti alloy. An in vivo study of nanocoated Ti implant surfaces showed enhanced bone integration, implying that the nanostructures may encourage osteoinduction [96].

5.2. Thermal Oxidation

Thermal oxidation (TO) is a simple and low-cost nanofabrication technique to generate nanostructured surfaces on titanium metal and its alloys in which growth of the nanostructures is dependent on the controlled oxidation of the substrate at high temperatures ranging from 400 to 900 °C within a carbon-containing atmosphere. At standard ambient temperature and pressure, titanium will spontaneously react with oxygen to form a stable oxide layer that generates a corrosion resistant barrier [97]. In general, TO of titanium or its alloys takes place in a tube furnace purged with carbon-containing vapour such as acetone and Ar, which is maintained at high temperatures for some time. As-synthesized nanostructured surfaces display superhydrophobic wetting, owing to a carbon shell that forms around the TiO_2 core [98]. Superhydrophobicity could be expected to prevent the attachment of mammalian cells, thereby reducing osseointegration [23]. To prevent against this, post-annealing can be applied to remove carbon, leaving only TiO_2 nanostructures that enhance osseointegration [80,82]. Much like the AH and other fabrication techniques discussed in this review, TO offers excellent versatility in terms of the design of the nanostructures. The parameters that control the nanostructures include the type of substrate (i.e., pure Ti or Ti alloy), Ar/acetone flow rate, holding temperature and time and post-treatment. Similar to the AH process, nanostructures fabricated using TO mimic the dragonfly wing surface (Figure 4B).

TO titanium (TOT) surfaces have been reported to show promising antibacterial properties [47,93]. By using a metabolic assay, PrestoBlue™, Sjöström et al. reported a 40% reduction in *E. coli* viability on TOT surfaces after 2 h of static incubation. The nanospikes had a diameter of 20 nm and a height of 1–2 µm [93]. More recently, Jenkins et al. found that TOT surfaces produced at 850 °C for 5 min mediated antibacterial effects against both Gram-negative (*E. coli*, *K. pneumoniae*) and Gram-positive (*S. aureus*) bacteria when tested over 10 h of static incubation using a BacTiter-Glo™ viability assay [47]. Enhanced osteogenic properties have also been reported for TOT surfaces. Wang et al. reported enhanced proliferation of bone marrow mesenchymal stem cells (hMSCs) on TOT surfaces compared to the control surface. Full confluence was observed on each surface after 7 days but significantly higher expression of osteogenic-related genes (e.g., alkaline phosphate, osteocalcin, osteopontin, bone sialoprotein) after 14 days and better matrix mineralisation after 21 days was seen on the surface with long nanostructures. Tan et al. also reported enhanced expression of osteogenic-related genes on TOT surfaces [99]. Using a rat calvarial model, computer tomography analysis revealed that there was an increased bone volume on the interface between a TOT surface and calvarial bone after 8 weeks relative to control [99].

5.3. Glancing Angle Deposition

Glancing angle deposition (GLAD) is a physical vapor deposition technique that is capable of fabricating nanostructured surfaces on planar and non-planar surfaces. This tuneable nanofabrication technique utilises oblique angle deposition and substrate rotation to engineer nanostructured surfaces [100]. In comparison to the other fabrication techniques mentioned, GLAD allows a high degree of precision control to uniquely designed micro and nanostructures, which is sometimes called "sculptured thin films" (Figure 4C). It is possible to generate a biomimetic surface that resembles the cicada wing surface with uniform height and distribution.

The incoming vapor flux is key to generating the desirable ballistic shadowing that is the underlying principle for this technique. For example, if the angular spread of the vapor flux is large, shadows generated on the substrate will be scattered and poorly defined. In general, to achieve collimated vapor flux, the distance between vapour source and the substrate must be large. As for other highly controllable nanofabrication techniques, GLAD requires great precision involving multiple parameters. For instance, the growth of nanostructures depends on the shadows between columns, vacuum environment, deposition temperature, rate and pressure, as well as substrate type and preparation [101].

Several microbiology and stem cell studies using nanospikes fabricated using GLAD on titanium substrates have been published recently [102–105]. Zeigler et al. reported promising bactericidal effects of the nanospikes against *E. coli* and a significant improvement in promoting the osteogenic response of hMSCs compared to plasma roughened TiO_2 surfaces [105]. Motemani et al. reported different levels of hMSC growth on slanted, chevron and vertical structures on TiO_2 substrate [102]. This confirms the biocompatibility of nanostructures generated using GLAD. Similarly, Sengstock et al. reported bactericidal activity against *E. coli* and successful attachment of hMSCs and leukocytes on the vertical structures of TiO_2 generated using GLAD [103]. The "race for the surface" experiment by Alvarez et al. using nanostructured surfaces showed that the nanocoated Ti implant supported the proliferation and spreading of MC3T3-E1 cells, despite the presence of *S. aureus* at a seeded ratio of 1:100. Furthermore, levels of proliferation and spreading of the MC3T3-E1 cells were significantly higher on the nanostructured surfaces compared to the uncoated TiO_2 surface, with or without the presence of *S. aureus* [104].

5.4. Reactive Ion Etching

Reactive ion etching (RIE) is commonly used to generate nanostructured surfaces on polymer and silicon surfaces. It is often combined with mask or colloidal lithography to control the size and shape of the nanostructures. Recently, a novel nanomaterial surface called black titanium was fabricated on a pure Ti substrate through a process called inductive coupled plasma reactive ion etching (ICP-RIE) [48,106]. ICP-RIE is a form of the RIE system that uses very high density plasma, generated with a radio frequency powered magnetic field as the etching source and chlorine as an etchant. The etching profile from an ICP source generated anisotropic nanoarrays but when combined with RIE, the enhanced control near the surface enabled the generation of both isotropic and anisotropic features [107]. The nanotopography of an etched Ti substrate mimics the dragonfly wing and longer etching times can result in a surface similar to the "niche" type surface generated using the AH method (Figure 4D).

Recently, a systematic study investigated the effects of etching conditions on the corresponding length of nanopillars, wettability of the surfaces and mechanical properties of the nanostructures [106]. It was reported that an increase in etching time, temperature, ICP power, RF power and Cl_2 pressure results in an increase in nanopillar length, while the Ti surfaces become more hydrophilic as the etching time, ICP power and RF power are increased. Both elastic modulus and hardness of the nanostructures increase as the chamber pressure increases, with a maximum elastic modulus and hardness of 30 and 2300 MPa, respectively, reported [106].

In another study, Hasan et al. compared the bactericidal activity and cytocompatibility of 3 different black titanium surfaces bearing approximately 1 µm protruded nanostructures [48]. Each black Ti surface had a different roughness due to different etching times. They reported significant bactericidal activity (over 90% death of the adherent cells) over a 4 h incubation period using several species of Gram-negative bacteria, while over 75% killing was reported for *S. aureus* after 24 h. They also tested the attachment and proliferation of hMSCs and osteogenic commitment of the stem cells on the black Ti surfaces and reported promising results, with ALP expression significantly higher in the hMSCs on the black Ti surface compared to the flat Ti surface.

6. Discussion

6.1. Scalability and Applicability of Nanofabrication Techniques for Medical Implants

All four nanofabrication techniques discussed here are capable of modifying the surface of a titanium implant with a high degree of design tunability. For translational purposes, other factors such as scalability and applicability must also be considered. Given the current trend in the development of 3D printing (3DP) technology, more orthopaedic and dental implant designs are incorporating 3D porous or lattice structures due to their advantages of better mechanical match to bone and improved osteointegration. It is therefore desirable to have a fabrication technique that could generate nanotopographies directly onto 3D porous implants. In this aspect, the AH and TO processes have the advantage of generating protruding nanostructured surfaces on any 3D surface, including inside the pores in 3DP implants. GLAD or RIE produce nanostructures by deposition or etching on either 2D planar or 3D non-planar surfaces but both require vacuum conditions and it is difficult to generate nanostructures inside pores. With regards to scalability, AH and TO processes are more amenable to batch processing, for which the substrates can be treated in a large autoclave container or tube furnace, respectively.

6.2. Eukaryotic Versus Prokaryotic Race for the Surface

The "race for the surface" concept between prokaryotes and eukaryotes describes the importance of host cell integration with the implant surface to protect against colonisation by microorganisms [79,108]. If the host tissue "wins" the race, osteointegration will be successful. However, if the microorganism colonises the implant surface before the host cells, a biofilm will develop, leading to severe infection and failure of the implant. Bacteria have also been shown to inhibit the spread and proliferation of osteoblastic cells, which indicates that it is not only a 'race' but rather a "fight for the surface" [6,109].

Briefly, there are two general approaches that can be used to help host cells win the race: (1) tuning the implant surfaces to selectively promote the attachment of mammalian cells or (2) inhibiting the adhesion of prokaryotes by killing them or deterring them from reaching the surface first. As discussed earlier, protruding nanostructured surfaces have the potential to exploit both approaches. Numerous studies have shown that it is possible for nanostructured surfaces to promote osteointegration whilst inhibiting bacterial growth.

6.3. Advantages and Disadvantages of Mechano-Biocidal Surfaces

The main advantage of mechano-biocidal surfaces is that they are unlikely to induce antimicrobial resistance (AMR). This is in contrast to existing biocide leaching surfaces, whose antimicrobial properties are dependent on antimicrobial release. For biocide leaching surfaces, antimicrobial release is dose-dependent, transient and subject to depletion over time, which could facilitate the development of AMR due to a sub-optimal release profile. In contrast, mechano-biocidal surfaces based on protruding nanostructures kill bacteria or inhibit biofilm formation upon contact and do not require specific biochemical targets. In addition, nanostructured surfaces offer the potential to be combined with bioactive dopants or other biomolecules such as antimicrobial peptides (AMPs) or ECM-mimicking

peptides to mediate synergistic effects that enhance their overall biological functionalities [110–112]. This could lead to the development of cell-instructive smart implants [6].

Despite their advantages, there are concerns over the robustness of nanostructures on the substrate, which raises the question as to whether or not the nanostructures could withstand invasive surgical procedures. There are also concerns regarding cytotoxicity. No studies to date have reported on the cytotoxicity of nanostructures when bound to the substrate but nanostructures in free form have been reported to exhibit some level of cytotoxicity towards mammalian cells [113]. It is also unclear whether or not nanostructured surfaces can remain effective, particularly with regards to their antimicrobial effects, following implantation and the inevitable adsorption of proteins from body fluids.

7. Conclusions and Outlook

With increasing demands for titanium-based medical implants, infections are inevitable and pose serious problems for the future. Furthermore, the growing threat of AMR means that we must use antibiotics more cautiously to treat prosthetic joint infections. It is critical, therefore, that we find novel methods to reduce bacterial infection of orthopaedic implants. Protruding nanostructured surfaces have gained interest as one potential solution due to their reported antibacterial and osteogenic properties. Our current understanding of nanotopographies suggests that their antibacterial properties are multifactorial. The mechano-bactericidal effects depend on the stretching of the bacterial cell membrane, which in turn depends on the nanotopographies and the mechanical properties of the bacterial cell wall. There is also recent evidence to indicate that protruding nanostructured surfaces are able to mediate bacterial cell impedance, fatal shear forces and induce an oxidative stress response in bacteria. However, better understanding of these mechanisms is still required to enable us to fully exploit the potential for protruding nanostructured surfaces to be used to design anti-infective orthopaedic implants. It will also allow surface design to be tailored for different medical implant applications. Finally, the design of different nanotopographies will require versatile nanofabrication techniques that have a high yield and are efficient and cost effective. This will ensure successful translation of the technology from research lab to clinical implementation in the real world.

Author Contributions: Writing—original draft preparation, M.I.I. and X.L.; writing—review and editing, M.I.I., B.S., J.J. and A.H.N.; Supervision, B.S. and A.H.N. All authors have read and agreed to the published version of the manuscript.

Funding: We would like to thank the financial support from the MRC (MR/S010343/1).

Acknowledgments: Bo Su would like to thank the EU H2020 MSCA RISE Bio-TUNE programme.

Conflicts of Interest: The authors declare no conflict of interest.

References

1. Liu, L.; Webster, T.J. Nanotechnology for reducing orthopedic implant infections: Synthesis, characterization, and properties. In *Orthopedic Biomaterials*; Li, B., Webster, T., Eds.; Springer: Berlin, Germany, 2017; pp. 31–62.
2. Jäger, M.; Jennissen, H.P.; Dittrich, F.; Fischer, A.; Köhling, H.L. Antimicrobial and osseointegration properties of nanostructured titanium orthopaedic implants. *Materials* **2017**, *10*, 1302. [CrossRef] [PubMed]
3. Ibrahim, M.Z.; Sarhan, A.A.D.; Yusuf, F.; Hamdi, M. Biomedical materials and techniques to improve the tribological, mechanical and biomedical properties of orthopedic implants—A review article. *J. Alloys Compd.* **2017**, *714*, 636–667. [CrossRef]
4. Tande, A.J.; Patel, R. Prosthetic joint infection. *Clin. Microbiol. Rev.* **2014**, *27*, 302–345. [CrossRef]
5. *National Joint Registry for England, Wales, Northern Ireland and Isle of Man, 6th Annual Report 2019*; National Joint Registry: London, UK, January 2019.
6. Mas-Moruno, C.; Su, B.; Dalby, M.J. Multifunctional coatings and nanotopographies: Toward cell instructive and antibacterial implants. *Adv. Healthc. Mater.* **2019**, *8*, 1801103. [CrossRef] [PubMed]
7. Souza, J.C.M.; Sordi, M.B.; Kanazawa, M.; Ravindran, S.; Henriques, B.; Silva, F.; Aparicio, C.; Cooper, L.F. Nano-scale modification of titanium implant surfaces to enhance osseointegration. *Acta Biomater.* **2019**, *94*, 112–131. [CrossRef]

8. Prasad, S.; Ehrensberger, M.; Gibson, M.P.; Kim, H.; Monaco, E.A., Jr. Biomaterial properties of titanium in dentistry. *J. Oral Biosci.* **2015**, *57*, 192–199. [CrossRef]
9. Sargolzaie, N.; Moeintaghavi, A.; Shojaie, H. Comparing the quality of life of patients requesting dental implants before and after implant. *Open Dent. J.* **2017**, *11*, 485. [CrossRef]
10. Catherine, D.; Koray, F.; Philip, F.; Stephen, H.; Craig, P.; David, S. *A Dentist's Guide To Implantology*; The Association of Dental Implantology: Richmond, VA, USA, 2012.
11. Raikar, S.; Talukdar, P.; Kumari, S.; Panda, S.K.; Oommen, V.M.; Prasad, A. Factors affecting the survival rate of dental implants: A retrospective study. *J. Int. Soc. Prev. Community Dent.* **2017**, *7*, 351. [CrossRef]
12. Passarelli, P.C.; De Leonardis, M.; Piccirillo, G.B.; Desantis, V.; Papa, R.; Rella, E.; Bonaviri, G.N.M.; Papi, P.; Pompa, G.; Pasquantonio, G.; et al. The effectiveness of chlorhexidine and air polishing system in the treatment of candida albicans infected dental implants: An experimental in vitro study. *Antibiotics* **2020**, *9*, 179. [CrossRef]
13. Di Murro, B.; Papi, P.; Passarelli, P.C.; D'Addona, A.; Pompa, G. Attitude in radiographic post-operative assessment of dental implants among italian dentists: A cross-sectional survey. *Antibiotics* **2020**, *9*, 234. [CrossRef]
14. Ribeiro, M.; Monteiro, F.J.; Ferraz, M.P. Infection of orthopedic implants with emphasis on bacterial adhesion process and techniques used in studying bacterial-material interactions. *Biomatter* **2012**, *2*, 176–194. [CrossRef] [PubMed]
15. Gallo, J.; Kolar, M.; Novotny, R.; Rihakova, P.; Tichá, V. Pathogenesis of prosthesis-related infection. *Biomed. Pap. Med. Fac. Univ. Palacky Olomouc. Czech Repub.* **2003**, *147*, 27–35. [CrossRef] [PubMed]
16. Burch, M.A.; Moriarty, T.F.; Kuehl, R.; Foster, A.; Morgenstern, M. Complications in orthopedic trauma surgery: Fracture-related infection. In *Racing for the Surface*; Li, B., Moriarty, T.F., Webster, T., Xing, M., Eds.; Springer: Berlin, Germany, 2020; pp. 33–56.
17. Flemming, H.-C.; Wingender, J.; Szewzyk, U.; Steinberg, P.; Rice, S.A.; Kjelleberg, S. Biofilms: An emergent form of bacterial life. *Nat. Rev. Microbiol.* **2016**, *14*, 563. [CrossRef] [PubMed]
18. Moran, E.; Byren, I.; Atkins, B.L. The diagnosis and management of prosthetic joint infections. *J. Antimicrob. Chemother.* **2010**, *65*, iii45–iii54. [CrossRef]
19. AshaRani, P.V.; Low Kah Mun, G.; Hande, M.P.; Valiyaveettil, S. Cytotoxicity and genotoxicity of silver nanoparticles in human cells. *ACS Nano* **2009**, *3*, 279–290. [CrossRef]
20. Hetrick, E.M.; Schoenfisch, M.H. Reducing implant-related infections: Active release strategies. *Chem. Soc. Rev.* **2006**, *35*, 780–789. [CrossRef]
21. Joost, U.; Juganson, K.; Visnapuu, M.; Mortimer, M.; Kahru, A.; Nõmmiste, E.; Joost, U.; Kisand, V.; Ivask, A. Photocatalytic antibacterial activity of nano-TiO_2 (anatase)-based thin films: Effects on Escherichia coli cells and fatty acids. *J. Photochem. Photobiol. B Biol.* **2015**, *142*, 178–185. [CrossRef]
22. Stewart, P.S. Antimicrobial tolerance in biofilms. *Microb. Biofilms* **2015**, 269–285. [CrossRef]
23. Mah, T.-F.C.; O'Toole, G.A. Mechanisms of biofilm resistance to antimicrobial agents. *Trends Microbiol.* **2001**, *9*, 34–39. [CrossRef]
24. Darouiche, R.O.O.; Weinstein, R.A. Device-associated infections: A macroproblem that starts with microadherence. *Clin. Infect. Dis.* **2001**, *33*, 1567–1572. [CrossRef]
25. Veerachamy, S.; Yarlagadda, T.; Manivasagam, G.; Yarlagadda, P.K.D.V. Bacterial adherence and biofilm formation on medical implants: A review. *Proc. Inst. Mech. Eng. Part H J. Eng. Med.* **2014**, *228*, 1083–1099. [CrossRef] [PubMed]
26. Bryers, J.D. Medical biofilms. *Biotechnol. Bioeng.* **2008**, *100*, 1–18. [CrossRef] [PubMed]
27. Renner, L.D.; Weibel, D.B. Physicochemical regulation of biofilm formation. *MRS Bull.* **2011**, *36*, 347–355. [CrossRef] [PubMed]
28. Bhushan, B.; Jung, Y.C.; Niemietz, A.; Koch, K. Lotus-like biomimetic hierarchical structures developed by the self-assembly of tubular plant waxes. *Langmuir* **2009**, *25*, 1659–1666. [CrossRef]
29. Mann, E.E.; Manna, D.; Mettetal, M.R.; May, R.M.; Dannemiller, E.M.; Chung, K.K.; Brennan, A.B.; Reddy, S.T. Surface micropattern limits bacterial contamination. *Antimicrob. Resist. Infect. Control* **2014**, *3*, 28. [CrossRef]
30. Sharklet. Sharklet—Products 2020. Available online: http://www.sharklet.com/our-products (accessed on 10 June 2020).

31. Fernández, I.C.S.; Van der Mei, H.C.; Metzger, S.; Grainger, D.W.; Engelsman, A.F.; Nejadnik, M.R.; Busschera, H.J. In vitro and in vivo comparisons of staphylococcal biofilm formation on a cross-linked poly (ethylene glycol)-based polymer coating. *Acta Biomater.* **2010**, *6*, 1119–1124. [CrossRef]
32. Kim, S.; Jung, U.T.; Kim, S.-K.; Lee, J.-H.; Choi, H.S.; Kim, C.-S.; Jeong, M.Y. Nanostructured multifunctional surface with antireflective and antimicrobial characteristics. *ACS Appl. Mater. Interfaces* **2015**, *7*, 326–331. [CrossRef]
33. Magin, C.M.; May, R.M.; Drinker, M.C.; Cuevas, K.H.; Brennan, A.B.; Reddy, S.T. Micropatterned protective membranes inhibit lens epithelial cell migration in posterior capsule opacification model. *Transl. Vis. Sci. Technol.* **2015**, *4*, 9. [CrossRef]
34. Ivanova, E.P.; Hasan, J.; Webb, H.K.; Truong, V.K.; Watson, G.S.; Watson, J.A.; Baulin, V.A.; Pogodin, S.; Wang, J.Y.; Tobin, M.J.; et al. Natural bactericidal surfaces: Mechanical rupture of Pseudomonas aeruginosa cells by cicada wings. *Small* **2012**, *8*, 2489–2494. [CrossRef]
35. Ball, P. Shark skin and other solutions. *Nature* **1999**, *400*, 507–509. [CrossRef]
36. Carman, M.L.; Estes, T.G.; Feinberg, A.W.; Schumacher, J.F.; Wilkerson, W.; Wilson, L.H.; Callow, M.E.; Callow, J.A.; Brennan, A.B. Engineered antifouling microtopographies—Correlating wettability with cell attachment. *Biofouling* **2006**, *22*, 11–21. [CrossRef] [PubMed]
37. Scardino, A.J.; Zhang, H.; Cookson, D.J.; Lamb, R.N.; de Nys, R. The role of nano-roughness in antifouling. *Biofouling* **2009**, *25*, 757–767. [CrossRef] [PubMed]
38. Ivanova, E.P.; Hasan, J.; Webb, H.K.; Gervinskas, G.; Juodkazis, S.; Truong, V.K.; Wu, A.H.F.; Lamb, R.N.; Baulin, V.A.; Watson, G.S. Bactericidal activity of black silicon. *Nat. Commun.* **2013**, *4*, 1–7. [CrossRef] [PubMed]
39. Kelleher, S.M.; Habimana, O.; Lawler, J.; O'reilly, B.; Daniels, S.; Casey, E.; Cowley, A. Cicada wing surface topography: An investigation into the bactericidal properties of nanostructural features. *ACS Appl. Mater. Interfaces* **2016**, *8*, 14966–14974. [CrossRef] [PubMed]
40. Bandara, C.D.; Singh, S.; Afara, I.O.; Wolff, A.; Tesfamichael, T.; Ostrikov, K.; Oloyede, A. Bactericidal effects of natural nanotopography of dragonfly wing on escherichia coli. *ACS Appl. Mater. Interfaces* **2017**, *9*, 6746–6760. [CrossRef]
41. Minoura, K.; Yamada, M.; Mizoguchi, T.; Kaneko, T.; Nishiyama, K.; Ozminskyj, M.; Koshizuka, T.; Ikuo, W.; Tatsuo, S. Antibacterial effects of the artificial surface of nanoimprinted moth-eye film. *PLoS ONE* **2017**, *12*, e0185366. [CrossRef]
42. Li, X.; Cheung, G.S.; Watson, G.S.; Watson, J.A.; Lin, S.; Schwarzkopf, L.; Green, D.W. The nanotipped hairs of gecko skin and biotemplated replicas impair and/or kill pathogenic bacteria with high efficiency. *Nanoscale* **2016**, *8*, 18860–18869. [CrossRef]
43. Diu, T.; Faruqui, N.; Sjöström, T.; Lamarre, B.; Jenkinson, H.F.; Su, B.; Ryadnov, M.G. Cicada-inspired cell-instructive nanopatterned arrays. *Sci. Rep.* **2014**, *4*. [CrossRef]
44. Dickson, M.N.; Liang, E.I.; Rodriguez, L.A.; Vollereaux, N.; Yee, A.F. Nanopatterned polymer surfaces with bactericidal properties. *Biointerphases* **2015**, *10*, 021010. [CrossRef]
45. Hazell, G.; Fisher, L.E.; Murray, W.A.; Nobbs, A.H.; Su, B. Bioinspired bactericidal surfaces with polymer nanocone arrays. *J. Colloid Interface Sci.* **2018**, *528*, 389–399. [CrossRef]
46. Hazell, G.; May, P.W.; Taylor, P.; Nobbs, A.H.; Welch, C.C.; Su, B.B. Studies of black silicon and black diamond as materials for antibacterial surfaces. *Biomater. Sci.* **2018**, *6*, 1424–1432. [CrossRef] [PubMed]
47. Jenkins, J.; Mantell, J.; Neal, C.; Gholinia, A.; Verkade, P.; Nobbs, A.H.; Su, B. Antibacterial effects of nanopillar surfaces are mediated by cell impedance, penetration and induction of oxidative stress. *Nat. Commun.* **2020**, *11*, 1–14. [CrossRef] [PubMed]
48. Hasan, J.; Jain, S.; Chatterjee, K. Nanoscale topography on black titanium imparts multi-biofunctional properties for orthopedic applications. *Sci. Rep.* **2017**, *7*. [CrossRef] [PubMed]
49. Linklater, D.P.; Nguyen, H.K.D.; Bhadra, C.M.; Juodkazis, S.; Ivanova, E.P. Influence of nanoscale topology on bactericidal efficiency of black silicon surfaces. *Nanotechnology* **2017**, *28*, 245301. [CrossRef]
50. Tripathy, A.; Sen, P.; Su, B.; Briscoe, W.H. Natural and bioinspired nanostructured bactericidal surfaces. *Adv. Colloid Interface Sci.* **2017**, *248*, 85–104. [CrossRef] [PubMed]
51. Pogodin, S.; Hasan, J.; Baulin, V.A.; Webb, H.K.; Truong, V.K.; Nguyen, T.H.P.; Boshkovik, V.; Fluke, C.J.; Watson, G.S.; Watson, J.A. Biophysical model of bacterial cell interactions with nanopatterned cicada wing surfaces. *Biophys. J.* **2013**, *104*, 835–840. [CrossRef]

52. Xue, F.; Liu, J.; Guo, L.; Zhang, L.; Li, Q. Theoretical study on the bactericidal nature of nanopatterned surfaces. *J. Theor. Biol.* **2015**, *385*, 1–7. [CrossRef]
53. Li, X. Bactericidal mechanism of nanopatterned surfaces. *Phys. Chem. Chem. Phys.* **2015**, *18*, 1311–1316. [CrossRef]
54. Wu, S.; Zuber, F.; Maniura-Weber, K.; Brugger, J.; Ren, Q. Nanostructured surface topographies have an effect on bactericidal activity. *J. Nanobiotechnol.* **2018**, *16*, 20. [CrossRef]
55. Watson, G.S.; Green, D.W.; Watson, J.A.; Zhou, Z.; Li, X.; Cheung, G.S.P.; Gellender, M. A simple model for binding and rupture of bacterial cells on nanopillar surfaces. *Adv. Mater. Interfaces* **2019**, *6*, 1801646. [CrossRef]
56. Velic, A.; Tesfamichael, T.; Li, Z. Yarlagadda PKD V. Parametric study on nanopattern bactericidal activity. *Procedia Manuf.* **2019**, *30*, 514–521. [CrossRef]
57. Ayazi, M.; Ebrahimi, N.G.; Nodoushan, E.J. Bacterial adhesion reduction on the surface with a simulated pattern: An insight into extrand model. *Int. J. Adhes. Adhes.* **2019**, *88*, 66–73. [CrossRef]
58. Vadillo-Rodríguez, V.; Dutcher, J.R. Viscoelasticity of the bacterial cell envelope. *Soft Matter* **2011**, *7*, 4101–4110. [CrossRef]
59. Hori, K.; Matsumoto, S. Bacterial adhesion: From mechanism to control. *Biochem. Eng. J.* **2010**, *48*, 424–434. [CrossRef]
60. Li, X.; Chen, T. Enhancement and suppression effects of a nanopatterned surface on bacterial adhesion. *Phys. Rev. E* **2016**, *93*, 52419.
61. Olivi, M.; Zanni, E.; De Bellis, G.; Talora, C.; Sarto, C.; Palleschi, M.S.; Flahaut, C.; Monthioux, E.; Papino, M.; Uccelletti, S. Inhibition of microbial growth by carbon nanotube networks. *Nanoscale* **2013**, *5*, 9023–9029. [CrossRef]
62. Sahoo, S.; Rao, K.K.; Suraishkumar, G.K. Reactive oxygen species induced by shear stress mediate cell death in Bacillus subtilis. *Biotechnol. Bioeng.* **2006**, *94*, 118–127. [CrossRef]
63. Shah, F.A.; Thomsen, P.; Palmquist, A. Osseointegration and current interpretations of the bone-implant interface. *Acta Biomater.* **2019**, *84*, 1–15. [CrossRef]
64. Puleo, D.A.; Nanci, A. Understanding and controlling the bone–implant interface. *Biomaterials* **1999**, *20*, 2311–2321. [CrossRef]
65. Thompson, G.J.; Puleo, D.A. Effects of sublethal metal ion concentrations on osteogenic cells derived from bone marrow stromal cells. *J. Appl. Biomater.* **1995**, *6*, 249–258. [CrossRef]
66. Palmquist, A.; Omar, O.M.; Esposito, M.; Lausmaa, J.; Thomsen, P. Titanium oral implants: Surface characteristics, interface biology and clinical outcome. *J. R. Soc. Interface* **2010**, *7*, S515–S527. [CrossRef]
67. Karazisis, D.; Petronis, S.; Agheli, H.; Emanuelsson, L.; Norlindh, B.; Johansson, A.; Rasmusson, L.; Thomsen, P.; Omar, O. The influence of controlled surface nanotopography on the early biological events of osseointegration. *Acta Biomater.* **2017**, *53*, 559–571. [CrossRef] [PubMed]
68. Karazisis, D.; Ballo, A.M.; Petronis, S.; Agheli, H.; Emanuelsson, L.; Thomsen, P.; Omar, O. The role of well-defined nanotopography of titanium implants on osseointegration: Cellular and molecular events in vivo. *Int. J. Nanomed.* **2016**, *11*, 1367–1382. [CrossRef] [PubMed]
69. Sjöström, T.; Dalby, M.J.; Hart, A.; Tare, R.; Oreffo, R.O.C.; Su, B. Fabrication of pillar-like titania nanostructures on titanium and their interactions with human skeletal stem cells. *Acta Biomater.* **2009**, *5*, 1433–1441. [CrossRef]
70. Ahn, J.; Son, S.J.; Min, J. The control of cell adhesion on a PMMA polymer surface consisting of nanopillar arrays. *J. Biotechnol.* **2013**, *164*, 543–548. [CrossRef]
71. Lim, J.Y.; Hansen, J.C.; Siedlecki, C.A.; Runt, J.; Donahue, H.J. Human foetal osteoblastic cell response to polymer-demixed nanotopographic interfaces. *J. R. Soc. Interface* **2005**, *2*, 97–108. [CrossRef]
72. Dalby, M.J.; Andar, A.; Nag, A.; Affrossman, S.; Tare, R.; McFarlane, S.; Oreffo, R.O.C. Genomic expression of mesenchymal stem cells to altered nanoscale topographies. *J. R. Soc. Interface* **2008**, *5*, 1055–1065. [CrossRef]
73. Dalby, M.J.; McCloy, D.; Robertson, M.; Agheli, H.; Sutherland, D.; Affrossman, S.; Oreffo, R.O.C. Osteoprogenitor response to semi-ordered and random nanotopographies. *Biomaterials* **2006**, *27*, 2980–2987. [CrossRef]
74. Yu, P.; Zhu, X.; Wang, X.; Wang, S.; Li, W.; Tan, G.; Zhang, Y.; Ning, C. Periodic nanoneedle and buffer zones constructed on a titanium surface promote osteogenic differentiation and bone calcification in vivo. *Adv. Healthc. Mater.* **2016**, *5*, 364–372. [CrossRef]

75. McNamara, L.E.; Sjöström, T.; Burgess, K.E.V.; Kim, J.J.W.; Liu, E.; Gordonov, S.; Moghe, P.V.; Meek, R.M.D.; Oreffo, R.O.C.; Su, B. Skeletal stem cell physiology on functionally distinct titania nanotopographies. *Biomaterials* **2011**, *32*, 7403–7410. [CrossRef]
76. Silverwood, R.K.; Fairhurst, P.G.; Sjöström, T.; Welsh, F.; Sun, Y.; Li, G.; Yu, B.; Young, P.S.; Su, B.; Meek, R.M.D.; et al. Analysis of osteoclastogenesis/osteoblastogenesis on nanotopographical titania surfaces. *Adv. Healthc. Mater.* **2016**, *5*, 947–955. [CrossRef] [PubMed]
77. Papi, P.; Raco, A.; Pranno, N.; Di Murro, B.; Passarelli, P.C.; D'Addona, A.; Pompa, G.; Barbieri, M. Salivary levels of titanium, nickel, vanadium, and arsenic in patients treated with dental implants: A case-control study. *J. Clin. Med.* **2020**, *9*, 1264. [CrossRef] [PubMed]
78. Meyer, A.D.; Aten, K.; Krause, A.J.; Metzger, M.L.; Holloway, S.S. Creating a university technology commercialisation programme: Confronting conflicts between learning, discovery and commercialisation goals. *Int. J. Entrep. Innov. Manag.* **2011**, *13*, 179–197. [CrossRef]
79. Busscher, H.J.; Van Der Mei, H.C.; Subbiahdoss, G.; Jutte, P.C.; Van Den Dungen, J.J.A.M.; Zaat, S.A.J.; Schultz, M.J.; Grainger, D.W. Biomaterial-associated infection: Locating the finish line in the race for the surface. *Sci. Transl. Med.* **2012**, *4*, 153rv10. [CrossRef]
80. Fernandez-Moure, J.S. Lost in translation: The gap in scientific advancements and clinical application. *Front. Bioeng. Biotechnol.* **2016**, *4*, 43. [CrossRef]
81. Wong, C.L.; Tan, Y.N.; Mohamed, A.R. A review on the formation of titania nanotube photocatalysts by hydrothermal treatment. *J. Environ. Manag.* **2011**, *92*, 1669–1680. [CrossRef]
82. Lee, J.; Kang, B.S.; Hicks, B.; Chancellor, T.F., Jr.; Chu, B.H.; Wang, H.T.; Keselowsky, B.G.; Ren, F.; Lele, T.P. The control of cell adhesion and viability by zinc oxide nanorods. *Biomaterials* **2008**, *29*, 3743–3749. [CrossRef]
83. Shim, J.B.; Chang, H.; Kim, S.-O. Rapid hydrothermal synthesis of zinc oxide nanowires by annealing methods on seed layers. *J. Nanomater.* **2011**, *2011*. [CrossRef]
84. Joshi, U.A.; Yoon, S.; Baik, S.; Lee, J.S. Surfactant-free hydrothermal synthesis of highly tetragonal barium titanate nanowires: A structural investigation. *J. Phys. Chem. B* **2006**, *110*, 12249–12256. [CrossRef]
85. Bao, N.; Shen, L.; Srinivasan, G.; Yanagisawa, K.; Gupta, A. Shape-controlled monocrystalline ferroelectric barium titanate nanostructures: From nanotubes and nanowires to ordered nanostructures. *J. Phys. Chem. C* **2008**, *112*, 8634–8642. [CrossRef]
86. Joshi, U.A.; Lee, J.S. Template-free hydrothermal synthesis of single-crystalline barium titanate and strontium titanate nanowires. *Small* **2005**, *1*, 1172–1176. [CrossRef] [PubMed]
87. Li, S.; Zhang, H.; Xu, J.; Yang, D. Hydrothermal synthesis of flower-like $SrCO_3$ nanostructures. *Mater. Lett.* **2005**, *59*, 420–422. [CrossRef]
88. Kim, T.-G.; Park, B. Synthesis and growth mechanisms of one-dimensional strontium hydroxyapatite nanostructures. *Inorg. Chem.* **2005**, *44*, 9895–9901. [CrossRef] [PubMed]
89. Damiati, L.; Eales, M.G.; Nobbs, A.H.; Su, B.; Tsimbouri, P.M.; Salmeron-Sanchez, M.; Dalby, M.J. Impact of surface topography and coating on osteogenesis and bacterial attachment on titanium implants. *J. Tissue Eng.* **2018**, *9*, 2041731418790694. [CrossRef] [PubMed]
90. Goriainov, V.; Hulsart-Billstrom, G.; Sjostrom, T.; Dunlop, D.G.; Su, B.; Oreffo, R.O.C. Harnessing nanotopography to enhance osseointegration of clinical orthopedic titanium implants—An in vitro and in vivo analysis. *Front. Bioeng. Biotechnol.* **2018**, *6*, 44. [CrossRef] [PubMed]
91. Cao, Y.; Su, B.; Chinnaraj, S.; Jana, S.; Bowen, L.; Charlton, S.; Duan, P.; Jakubovics, N.S.; Chen, J. Nanostructured titanium surfaces exhibit recalcitrance towards Staphylococcus epidermidis biofilm formation. *Sci. Rep.* **2018**, *8*, 1–13. [CrossRef]
92. Tsimbouri, P.M.; Fisher, L.; Holloway, N.; Sjostrom, T.; Nobbs, A.H.; Meek, R.M.D.; Su, B.; Dalby, M.J. Osteogenic and bactericidal surfaces from hydrothermal titania nanowires on titanium substrates. *Sci. Rep.* **2016**, *6*, 36857. [CrossRef]
93. Sjöström, T.; Nobbs, A.H.; Su, B. Bactericidal nanospike surfaces via thermal oxidation of Ti alloy substrates. *Mater. Lett.* **2016**, *167*, 22–26. [CrossRef]
94. Liu, B.; Boercker, J.E.; Aydil, E.S. Oriented single crystalline titanium dioxide nanowires. *Nanotechnology* **2008**, *19*, 505604. [CrossRef]
95. Yada, M.; Inoue, Y.; Uota, M.; Torikai, T.; Watari, T.; Noda, I.; Hotokebuchi, T. Plate, wire, mesh, microsphere, and microtube composed of sodium titanate nanotubes on a titanium metal template. *Langmuir* **2007**, *23*, 2815–2823. [CrossRef]

96. Umehara, H.; Kobatake, R.; Oki, Y.; Makihara, Y.; Kubo, T.; Tsuga, K. Histological and bone morphometric evaluation of osseointegration aspects by alkali hydrothermally-treated implants. *Appl. Sci.* **2018**, *8*, 635. [CrossRef]
97. De Viteri, V.S.; Fuentes, E. Titanium and titanium alloys as biomaterials. *Tribol.-Fundam. Adv.* **2013**, 155–181.
98. Jenkins, J.J. An Alternative Approach to Combat Antimicrobial Resistant Infections of Medical Implants And Devices. Ph.D. Thesis, University of Bristol, Bristol, UK, November 2019.
99. Wang, G.; Li, J.; Lv, K.; Zhang, W.; Ding, X.; Yang, G.; Liu, X.; Jiang, X. Surface thermal oxidation on titanium implants to enhance osteogenic activity and in vivo osseointegration. *Sci. Rep.* **2016**, *6*, 31769. [CrossRef] [PubMed]
100. Robbie, K.; Sit, J.C.; Brett, M.J. Advanced techniques for glancing angle deposition. *J. Vac. Sci. Technol. B Microelectron. Nanom. Struct. Process. Meas. Phenom.* **1998**, *16*, 1115–1122. [CrossRef]
101. Taschuk, M.T.; Hawkeye, M.M.; Brett, M.J. Glancing angle deposition. In *Handbook of Deposition Technologies for Films and Coatings*, 3rd ed.; Elsevier: Amsterdam, The Netherlands, 2010; pp. 621–678.
102. Motemani, Y.; Greulich, C.; Khare, C.; Lopian, M.; Buenconsejo, P.J.S.; Schildhauer, T.A.; Ludwig, A.; Köller, M. Adherence of human mesenchymal stem cells on Ti and TiO_2 nano-columnar surfaces fabricated by glancing angle sputter deposition. *Appl. Surf. Sci.* **2014**, *292*, 626–631. [CrossRef]
103. Sengstock, C.; Lopian, M.; Motemani, Y.; Borgmann, A.; Khare, C.; Buenconsejo, P.J.S.; Schildhauer, T.A.; Ludwig, A.; Köller, M. Structure-related antibacterial activity of a titanium nanostructured surface fabricated by glancing angle sputter deposition. *Nanotechnology* **2014**, *25*, 195101. [CrossRef]
104. Alvarez, R.; Muñoz-Piña, S.; González, M.U.; Izquierdo-Barba, I.; Fernández-Martínez, I.; Rico, V.; Arcos, D.; García-Valenzuela, A.; Palmero, A.; Vallet-Regi, M.; et al. Antibacterial nanostructured ti coatings by magnetron sputtering: From laboratory scales to industrial reactors. *Nanomaterials* **2019**, *9*, 1217. [CrossRef]
105. Ziegler, N.; Sengstock, C.; Mai, V.; Schildhauer, T.A.; Köller, M.; Ludwig, A. Glancing-angle deposition of nanostructures on an implant material surface. *Nanomaterials* **2019**, *9*, 60. [CrossRef]
106. Ganjian, M.; Modaresifar, K.; Zhang, H.; Hagedoorn, P.-L.; Fratila-Apachitei, L.E.; Zadpoor, A.A. Reactive ion etching for fabrication of biofunctional titanium nanostructures. *Sci. Rep.* **2019**, *9*, 1–20. [CrossRef]
107. Shah, A.P.; Laskar, M.R.; Azizur Rahman, A.; Gokhale, M.R.; Bhattacharya, A. Inductively coupled plasma–reactive ion etching of c-and a-plane AlGaN over the entire Al composition range: Effect of BCl3 pretreatment in Cl2/Ar plasma chemistry. *J. Vac. Sci. Technol. A Vac. Surf. Films* **2013**, *31*, 61305. [CrossRef]
108. Pham, V.T.H.; Truong, V.K.; Orlowska, A.; Ghanaati, S.; Barbeck, M.; Booms, P.; Fulcher, A.J.; Bhadra, C.M.; Buividas, R.; Baulin, V. "Race for the surface": Eukaryotic cells can win. *ACS Appl. Mater. Interfaces* **2016**, *8*, 22025–22031. [CrossRef]
109. Hoyos-Nogués, M.; Velasco, F.; Ginebra, M.-P.; Manero, J.M.; Gil, F.J.; Mas-Moruno, C. Regenerating bone via multifunctional coatings: The blending of cell integration and bacterial inhibition properties on the surface of biomaterials. *ACS Appl. Mater. Interfaces* **2017**, *9*, 21618–21630. [CrossRef] [PubMed]
110. Brandelli, A. Nanostructures as promising tools for delivery of antimicrobial peptides. *Mini Rev. Med. Chem.* **2012**, *12*, 731–741. [CrossRef] [PubMed]
111. Jäger, M.; Böge, C.; Janissen, R.; Rohrbeck, D.; Hülsen, T.; Lensing-Höhn, S.; Krauspe, R.; Herten, M. Osteoblastic potency of bone marrow cells cultivated on functionalized biometals with cyclic RGD-peptide. *J. Biomed. Mater. Res. Part A* **2013**, *101*, 2905–2914. [CrossRef]
112. Fraioli, R.; Tsimbouri, P.M.; Fisher, L.E.; Nobbs, A.H.; Su, B.; Neubauer, S.; Rechenmacher, F.; Kessler, H.; Ginebra, M.P.; Dalby, M.J.; et al. Towards the cell-instructive bactericidal substrate: Exploring the combination of nanotopographical features and integrin selective synthetic ligands. *Sci. Rep.* **2017**, *7*, 1–14. [CrossRef] [PubMed]
113. Cui, H.-F.; Vashist, S.K.; Al-Rubeaan, K.; Luong, J.H.T.; Sheu, F.-S. Interfacing carbon nanotubes with living mammalian cells and cytotoxicity issues. *Chem. Res. Toxicol.* **2010**, *23*, 1131–1147. [CrossRef] [PubMed]